TCOX9: TCS Metal Oxide Solutions Database

Database name:	TCS Metal Oxide Solutions Database	*Database acronym:*	TCOX
Database owner:	Thermo-Calc Software AB	*Database version:*	9.0

TCOX9 is a thermodynamic database for slags and oxides for use with Thermo-Calc and the add-on Diffusion Module (DICTRA) and/or Precipitation Module (TC-PRISMA). It is also used with the Process Metallurgy Calculator, which allows for the efficient setup of advanced calculations involving slag, metal and gas. Developed using the CALPHAD approach, TCOX9 is based on the critical evaluation of binary, ternary and important higher order systems which enables predictions to be made for multicomponent systems. The database is the result of a long-term collaboration with academia. The first release of the database was in August 1992.

Included Elements (25)

Al	Ar*	C	Ca	Co	Cr	Cu	F	Fe	Gd
La	Mg	Mn	Mo	Nb	Ni	O	P	S	Si
Ti	V	W	Y	Zr					

** Ar is only included in the gas phase.*

The intended application is for solid and liquid ionized materials, e.g. oxides or sulfides. This could be development of ceramics, slags, refractories, metallurgical processing (e.g. slag and liquid metal interactions), ESR slags, materials corrosion, Thermal Barrier Coatings (TBC), Yttria-Stabilised-Zirconia (YSZ), solid oxide fuel cell materials, sulfide formation, dephosphorization and desulfurization, but the database is of course not limited to this. Despite the name of the database, it can be used even for fluoride and sulfide systems without oxygen. The liquid phase is described from liquid metal to oxide and/or fluoride, i.e. no pure liquid oxygen or fluorine is modeled. For sulfur, the liquid phase is described all the way from metal to sulfur.

TCOX9 is developed in a CALPHAD spirit in order to give an accurate thermodynamic description of the multi-component systems of interest. In total, 260 binary systems and 244 ternary systems in this 25-element framework have been assessed to their full range of composition and temperature. In addition, TCOX9 also contains assessments of 118 pseudo-ternary oxide systems, 32 oxy-fluoride and oxy-sulfide systems, and some higher order systems as well. The systems and composition ranges which have been assessed are described below. The most accurate calculations will be obtained in or near these sub-systems and composition ranges.

However, intermetallic compounds and carbides are not included in the database. For solid phases, the TCOX9 database is compatible with TCFE Steels/Fe-Alloys Database, TCNI Ni-based Superalloys Database and SSOL Solutions Database. Thus, if needed, more metallic phases can be obtained by appending from TCFE, TCNI, SSOL and/or other appropriate databases. However, keep in mind that the LIQUID phase from other databases and the IONIC_LIQ phase from TCOX9 should never be simultaneously considered in the same defined system/calculation, as they both represent the liquid phase using two different models. The binary O- and S-systems can be calculated with the Console Mode BINARY module or Graphical Mode Binary Calculator in Thermo-Calc.

TCOX9 contains 382 phases in total. The liquid metal and slag (IONIC_LIQ) is described with the ionic two-sublattice liquid model [1985, Hillert; 1991, Sundman] using a single Gibbs energy curve. The advantage with the ionic two-sublattice model is that it allows a continuous description of a liquid which changes in character with composition. The model has successfully been used to describe liquid oxides, silicates, sulfides, fluorides as well as liquid short range order, molten salts and ordinary metallic liquids. At low level of oxygen, the model becomes equivalent to a substitutional solution model between metallic atoms.

Different composition sets of IONIC_LIQ designated by #1, #2 etc. (e.g. IONIC_LIQ#1) may be observed which often represent the metallic and ionized liquid phases. Different composition sets also describe miscibility gaps frequently found in e.g. silicate systems. The #n suffix (where n is an integer) is generated dynamically by Thermo-Calc when using global minimization and therefore the identification of the phases should be determined from their compositions.

TCOX9 also contains solid oxides, silicates, fluorides and sulfides, a gaseous mixture phase and solid solution alloy phases (FCC_A1, BCC_A2 etc). Many phases are modeled as solution phases (in all cases where it is meaningful). The solid solution phases such as spinel, mullite, corundum, halite, olivine, fluorite etc. are modeled within the framework of the Compound Energy Formalism (CEF) [2001, Hillert]. The complete list of phases is given in Phases Included in TCOX9.

Limits

As in the spirit of the CALPHAD method, predictions can be made for multicomponent systems by extrapolation into multicomponent space of data critically evaluated and assessed based on binary, ternary and in some cases higher order systems. However, critical calculations must always be verified by equilibrium experimental data; it is the user's responsibility to verify the calculations but Thermo-Calc Software AB is interested to know about any significant deviations in order to improve any future release.

Database Revision History

If you are interested in the revision history for this database, the information is available in the online help (from Thermo-Calc go to **Help>Online Help**) or in the release notes on our website.

TCOX9 Assessed Systems

These are the assessed systems in the full range of composition and temperature.

Assessed Metallic Systems

All metal-metal binaries except Ca-W, Ca-Zr, Gd-La, Gd-P, La-Nb, La-P, La-Si, Mg-P, P-V, P-W and P-Zr are assessed. Many ternary metallic systems are also assessed. No intermetallic phases are included in the database. If needed, more solid phases can be appended from TCFE (TCS Steel and Fe-alloys Database), TCNI (TCS Ni-based Superalloys Database), TCAL (TCS Al-based Alloy Database) or other appropriate databases.

Assessed Binary Oxide Systems

Al-O	Ca-O	Co-O	Cr-O	Cu-O	Fe-O	Gd-O	La-O	Mg-O	Mn-O
Mo-O	Nb-O	Ni-O	P-O	Si-O	Ti-O	V-O	W-O	Y-O	Zr-O

Assessed Ternary Oxide Systems, Me1-Me2-O

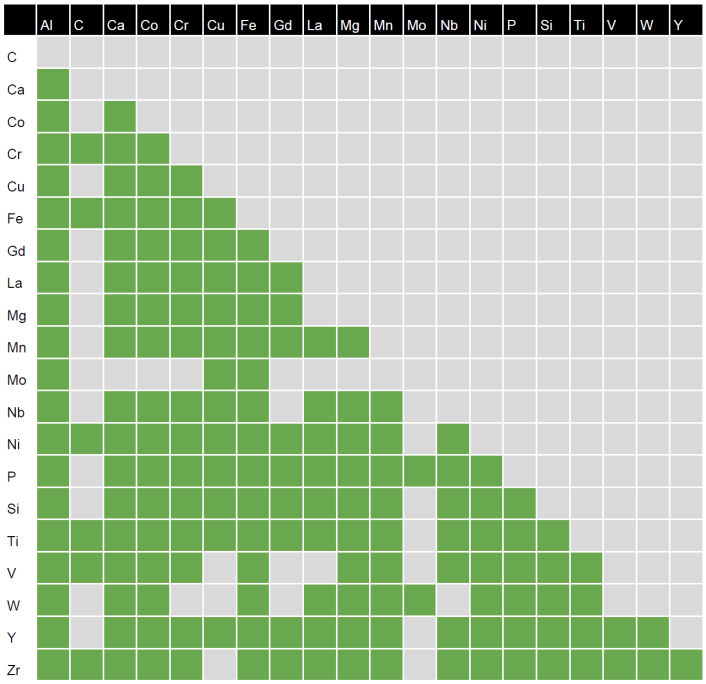

Assessed Quaternary Oxide Systems, Me1-Me2-Me3-O

Al-Ca-Co-O	Al-Ca-Cr-O	Al-Ca-Fe-O	Al-Ca-Gd-O	Al-Ca-Mg-O
Al-Ca-Mn-O	Al-Ca-Nb-O	Al-Ca-Ni-O	Al-Ca-O-P	Al-Ca-O-Si
Al-Ca-O-Ti	Al-Ca-O-Y	Al-Ca-O-Zr	Al-Co-O-Si	Al-Co-O-Ti
Al-Cr-Fe-O	Al-Cr-Mg-O	Al-Cr-O-Ti	Al-Cr-O-Y	Al-Cu-O-Si
Al-Fe-Mg-O	Al-Fe-Mn-O	Al-Fe-O-Si	Al-Fe-O-Ti	Al-Fe-O-Y
Al-Gd-O-Zr	Al-La-O-Y	Al-La-O-Zr	Al-Mg-O-P	Al-Mg-O-Si
Al-Mg-O-Ti	Al-Mg-O-Y	Al-Mg-O-Zr	Al-Mn-O-Si	Al-Mn-O-Ti
Al-Ni-O-Ti	Al-O-P-Si	Al-O-Si-Ti	Al-O-Si-Y	Al-O-Si-Zr
Al-O-Y-Zr	Ca-Co-O-Si	Ca-Cr-Fe-O	Ca-Cr-O-Si	Ca-Cu-Fe-O
Ca-Cu-O-Si	Ca-Fe-Mg-O	Ca-Fe-Mn-O	Ca-Fe-O-P	Ca-Fe-O-Si
Ca-Fe-O-Ti	Ca-Gd-O-Si	Ca-Mg-Mn-O	Ca-Mg-O-P	Ca-Mg-O-Si
Ca-Mg-O-Ti	Ca-Mg-O-Zr	Ca-Mn-O-P	Ca-Mn-O-Si	Ca-Mn-O-Y
Ca-Nb-O-Si	Ca-Ni-O-Si	Ca-O-P-Si	Ca-O-Si-Ti	Ca-O-Si-V
Ca-O-Si-Y	Ca-O-Si-Zr	Ca-O-Y-Zr	Co-Cr-O-Si	Co-Cr-O-Ti
Co-Cu-La-O	Co-Cu-O-Si	Co-Fe-La-O	Co-Fe-Mn-O	Co-Fe-O-P
Co-Fe-O-Si	Co-La-Ni-O	Co-Mg-O-Si	Co-Mn-O-Si	Co-Ni-O-Si
Cr-Fe-Mn-O	Cr-Fe-Ni-O	Cr-Fe-O-Si	Cr-Fe-O-Ti	Cr-Fe-O-Y
Cr-La-Mn-O	Cr-Mg-O-Si	Cr-Mg-O-Ti	Cr-Mn-Ni-O	Cr-Mn-O-Si
Cr-Mn-O-Ti	Cr-Ni-O-Si	Cr-Ni-O-Ti	Cu-Fe-O-Si	Cu-Mg-O-Si
Fe-Mg-O-Si	Fe-Mg-O-Ti	Fe-Mn-O-Si	Fe-Mn-O-Ti	Fe-Ni-O-Si

Fe-Ni-O-Ti	Fe-O-Si-Ti	Gd-La-O-Si	Gd-O-Si-Y	Gd-O-Si-Zr
La-O-Y-Zr	Mg-Mn-O-Si	Mg-Mn-O-Ti	Mg-Ni-O-Si	Mg-O-P-Si
Mg-O-Si-Ti	Mg-O-Si-V	Mg-O-Si-Y	Mg-O-Si-Zr	Mg-O-Y-Zr
Mn-Ni-O-V	Mn-O-Y-Zr	O-Ti-Y-Zr		

Assessed Higher Order Oxide Systems

Al-Ca-Co-O-Si	Al-Ca-Fe-O-Si	Al-Ca-Mg-O-Si	Al-Ca-Mg-O-Ti
Al-Ca-Mg-O-Zr	Al-Ca-O-Si-Y	Al-Fe-Mg-O-Si	Al-Fe-Mn-O-Si
Al-Gd-O-Y-Zr	Al-La-O-Y-Zr	Ca-Fe-Mg-O-Si	Ca-Mg-Ni-O-Si
Ca-Mg-O-P-Si	Gd-La-O-Y-Zr	C-Cr-Fe-Mn-Ni-O	

Assessed Binary Sulfide Systems

Al-S	Ca-S	Co-S	Cr-S	Cu-S	Fe-S	Gd-S
La-S	Mg-S	Mn-S	Mo-S	Nb-S	Ni-S	
Si-S	Ti-S	V-S	W-S	Y-S	Zr-S	

Assessed Ternary Sulfide Systems, Me1-Me2-S

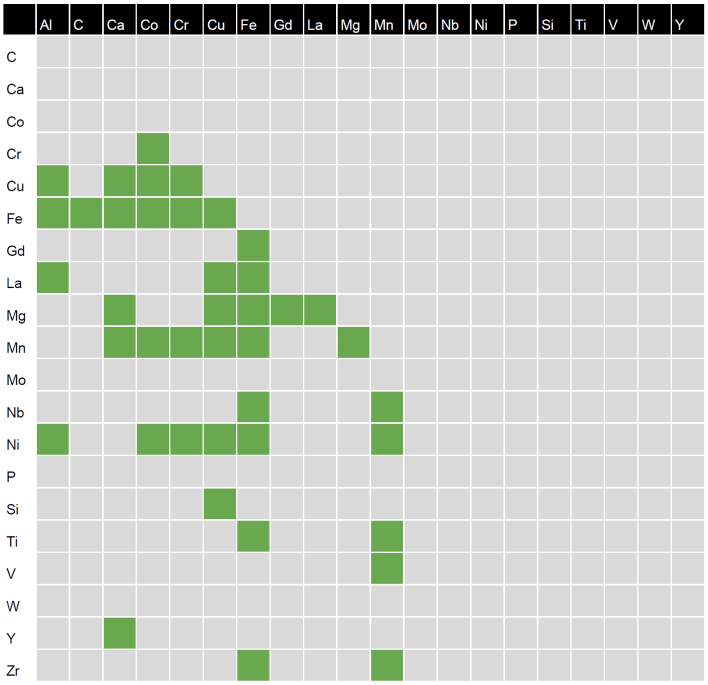

Assessed Oxy-sulfide Systems

Al-O-S	Ca-O-S	Co-O-S	Cr-O-S	Cu-O-S	Fe-O-S
Mg-O-S	Mn-O-S	O-S-Si	Al-Ca-O-S	Al-Mg-O-S	Al-Mn-O-S
Ca-Fe-O-S	Ca-Mg-O-S	Ca-O-S-Si	Cu-Fe-O-S	Fe-O-S-Si	Mg-O-S-Si
Mn-O-S-Si	Al-Ca-Mn-O-S				

Assessed Binary Fluoride Systems

AlF_3	Ca-F	CoF_2	CoF_3	CrF_2	CrF_3	CuF	CuF_2
FeF_2	FeF_3	GdF_3	LaF_3	MgF_2	MnF_2	MoF_4	
NbF_2	NbF_5	NiF_2	SiF_4	VF_2	YF_3	ZrF_4	

Assessed Ternary Fluoride Systems

Al-Ca-F	Al-F-Mg	Al-F-Zr	Ca-Co-F	Ca-Cr-F	Ca-Fe-F	Ca-F-Gd
Ca-F-La	Ca-F-Mg	Ca-F-Mn	Co-F-Gd	Co-F-Mg	Co-F-Ni	Fe-F-Ni
F-Gd-Mg	F-Gd-Y	F-La-Zr	F-Mg-La	F-Mg-Y		

Assessed Oxy-fluoride Systems

Al-F-O	Ca-F-O	Co-F-O	F-Mg-O	Al-Ca-F-O	Ca-F-Mg-O
Ca-Fe-F-O	Ca-F-O-P	Ca-F-O-Si	F-Mg-O-Si	Al-Ca-F-Mg-O	Al-Ca-F-O-Si

TCOX9 Calculation Examples

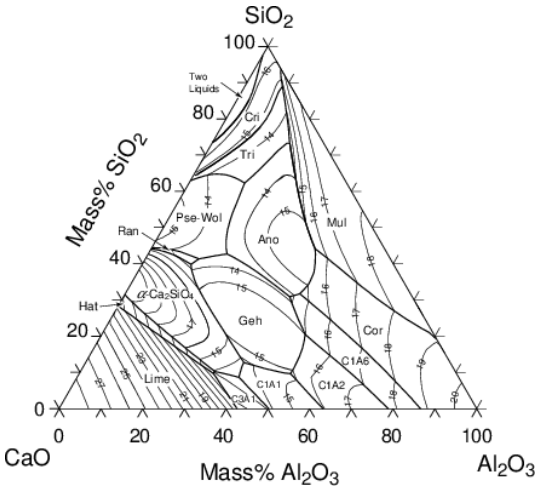

Figure 1: Calculated phase diagram of the CaO-Al_2O_3-SiO_2 system [2006, Mao]. Ano: anorthite, C1A1: $CaAl_2O_4$, C1A2: $CaAl_4O_7$, C1A6: $CaAl_{12}O_{19}$, C3A1: $Ca_3Al_2O_8$, Cor: corundum, Cri: cristobalite, Geh: gehlenite, Hat: hatrurite, Mul: mullite, Pse-Wol: pseudo-wollastonite, Ran: rankinite, Tri: tridymite.

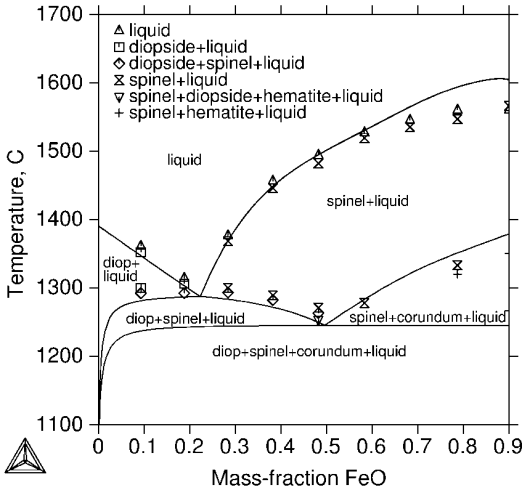

Figure 2: Calculated $CaMgSi_2O_6$ (diopside)-FeO_x section in air.

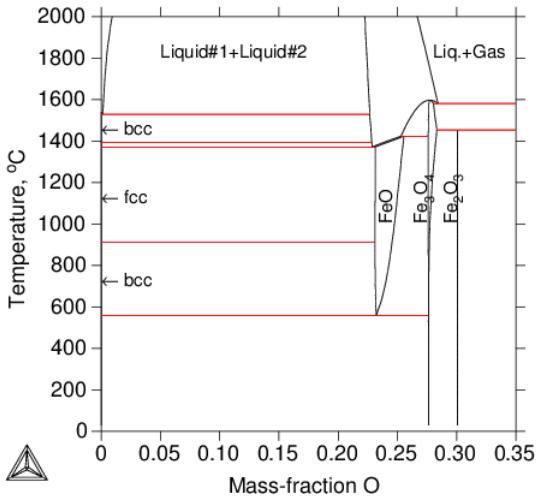

Figure 3: Calculated Fe-O phase diagram [1991, Sundman].

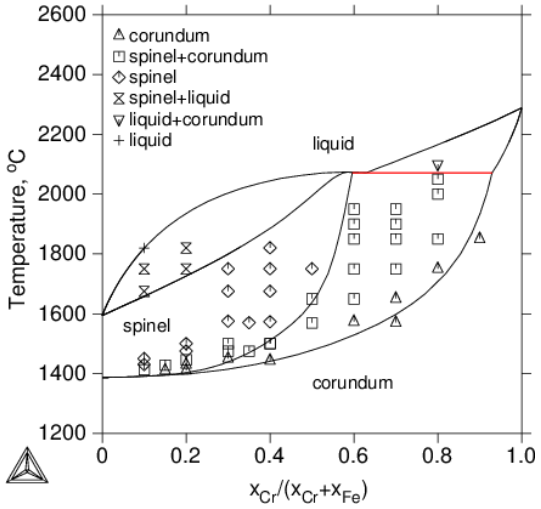

Figure 4: Calculated [2008, Kjellqvist] and experimental phase diagram of Cr-Fe-O in air [1960, Muan].

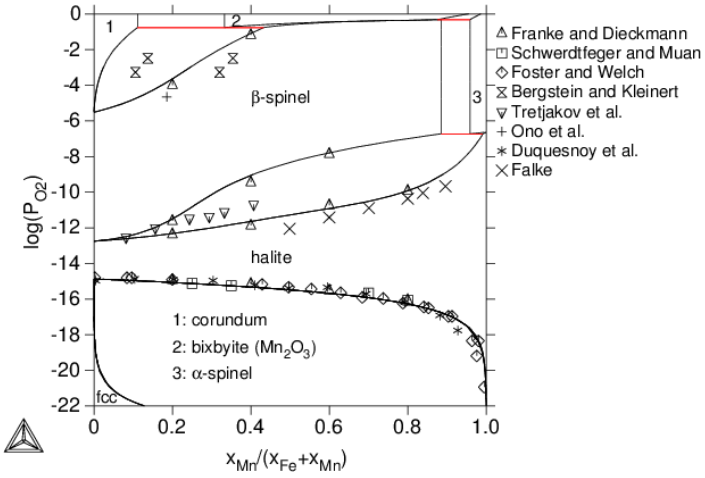

Figure 5: Calculated [2010, Kjellqvist] and experimental phase diagram of Fe-Mn-O at 1000 °C [1967, Schwerdt; 1990, Franke; 1956, Foster; 1971, Ono; 1975, Duquesnoy; 1987, Falke; 1964, Bergstein; 1965, Tretjakov].

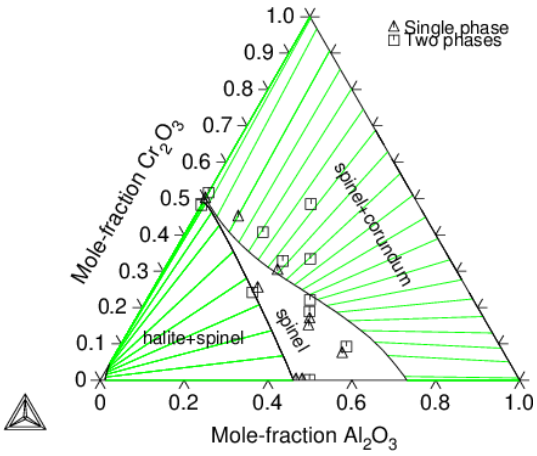

Figure 6: Calculated and experimental [1966, Greskovich] isothermal section of Al_2O_3-Cr_2O_3-MgO at 1700 °C and P_{O2}=1.

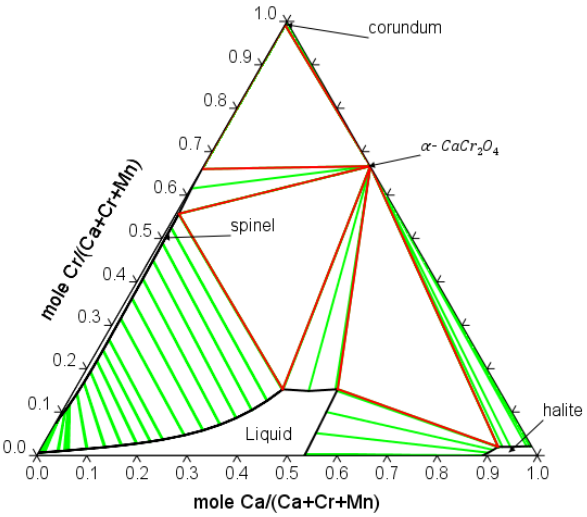

Figure 7: Isothermal section of CaO-Cr_2O_3-Mn_2O_3 calculated at 1600 °C in air.

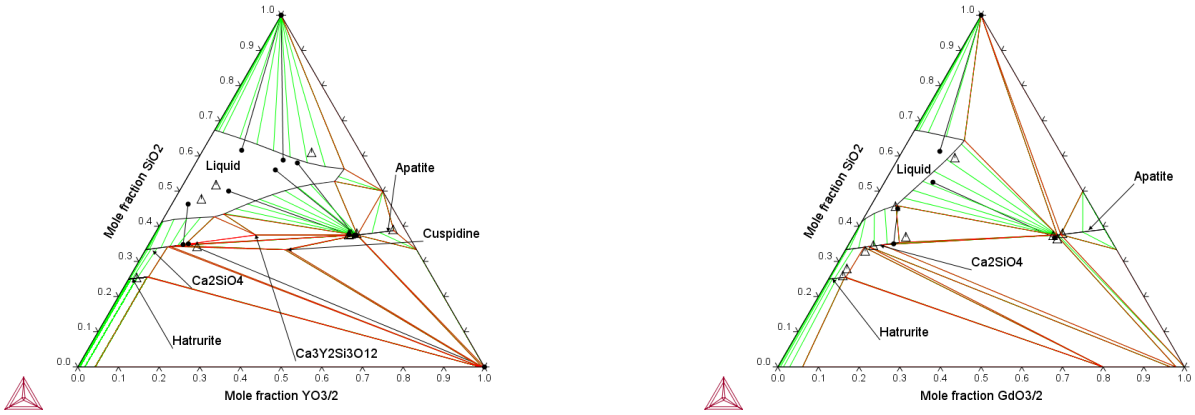

Figure 8: Calculated isothermal sections of CaO-SiO_2-$YO_{1.5}$ (left) and CaO-SiO_2-$GdO_{1.5}$ (right) at 1600 °C, compared to data on 3-phase corners and tie-lines from Poerschke [2017, 2016a, 2016b].

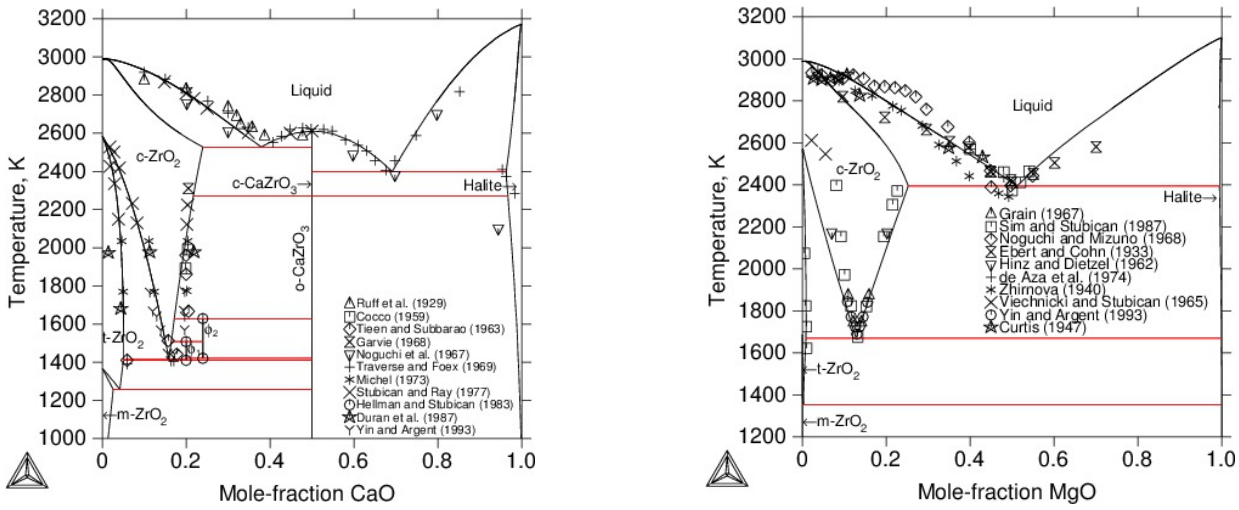

Figure 9: Calculated and experimental phase diagrams for CaO-ZrO_2 (left) and MgO-ZrO_2 (right) [see Figure 9 References].

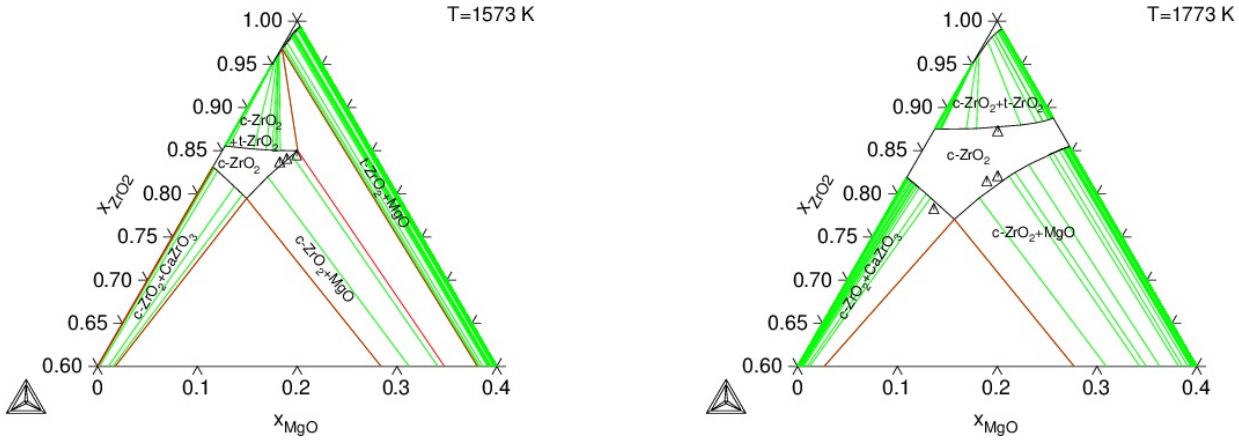

Figure 10: Isothermal sections of CaO-MgO-ZrO_2 calculated at 1300 °C and 1500 °C with experimental data [1993, Yin].

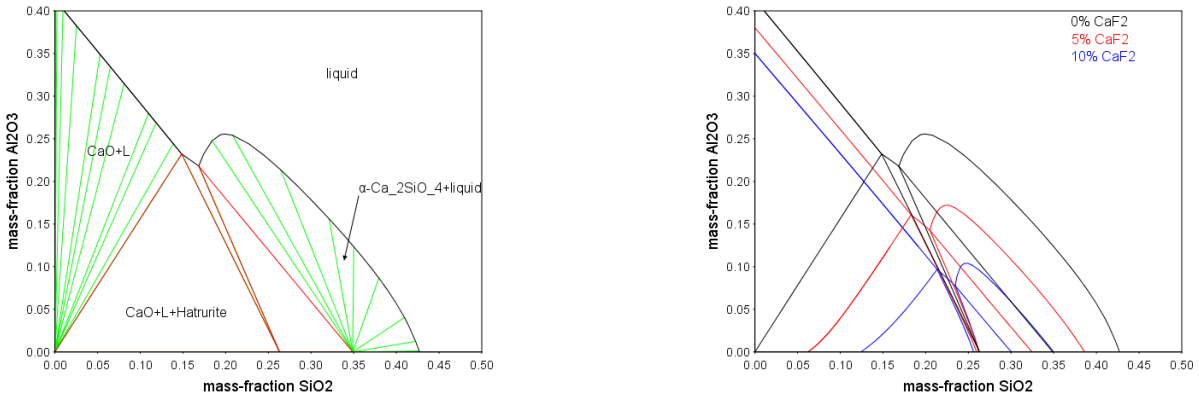

Figure 11: Calculated effect of CaF_2 on the Al_2O_3-CaO-SiO_2 system at 1600 °C.

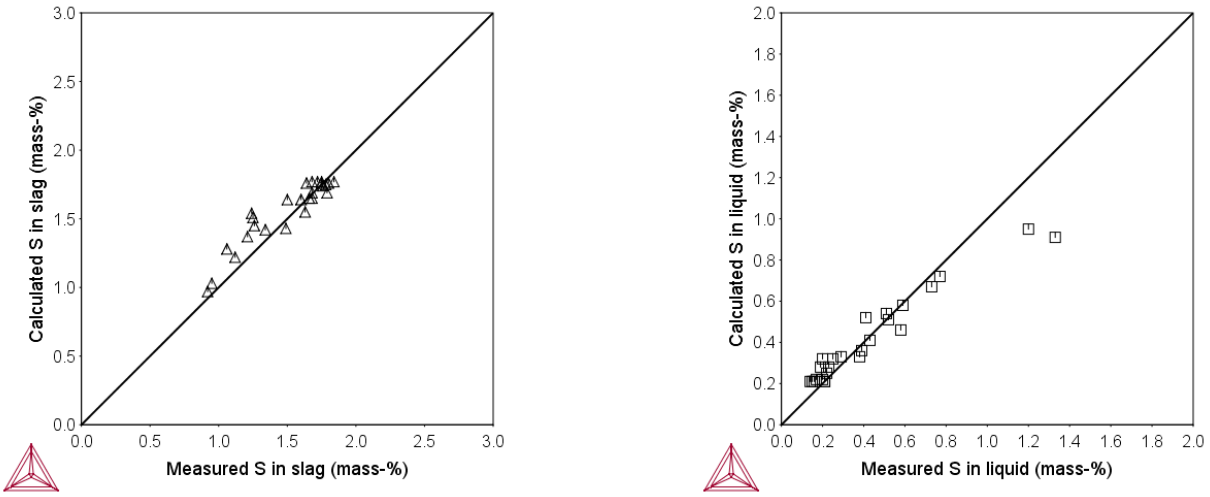

Figure 12: Sulfur in ladle slag. An impressive amount of sulfide capacity measurements have been made for a variety of slag systems over the years, but the results are very scattered. Allertz [2016] used a different method with equilibrium between copper and slag. Sulfur was added as Cu_2S. Different CMAS slags were then equilibrated with Cu and Cu_2S under controlled oxygen partial pressures. The equilibrium sulfur contents in the copper and slag were then analyzed.

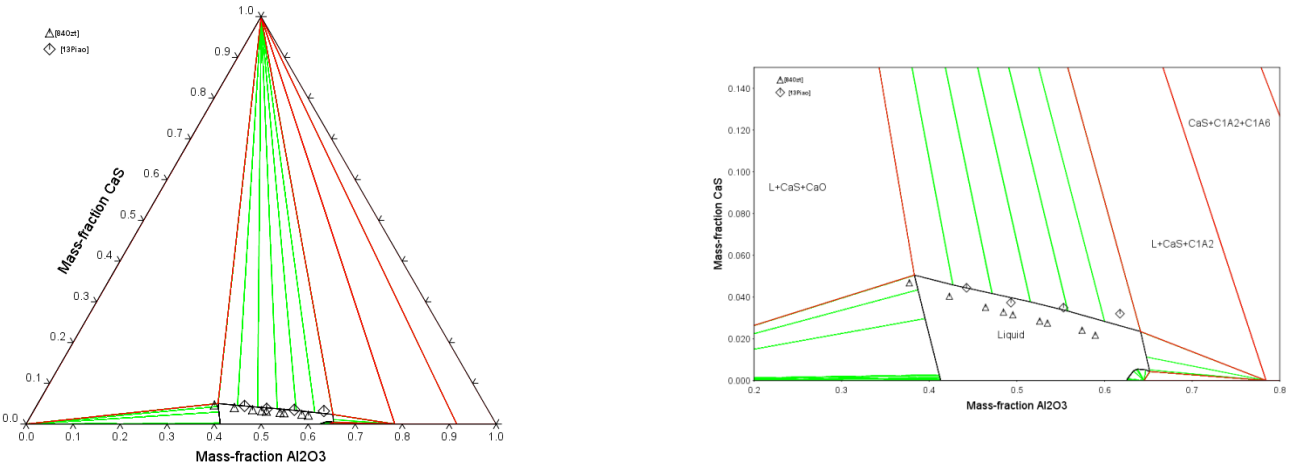

Figure 13: Isothermal section of the Al_2O_3-CaO-CaS system at 1600 °C with experimental data [1984, Ozturk; 2013, Piao].

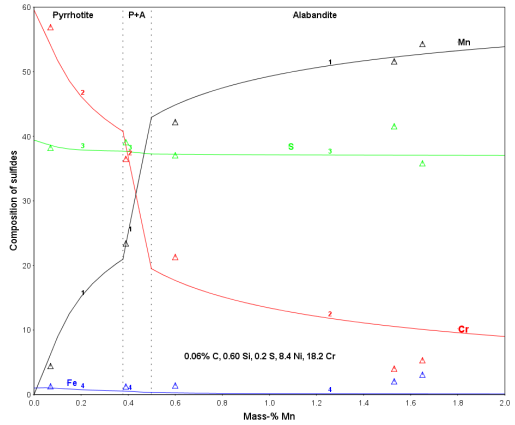

Figure 14: Calculated effect of inclusion composition of 18-8 stainless steel. The stability and composition of sulfides have been investigated [1980, Ono] at 1100 °C by varying the Mn concentraion of the steel: Fe - 0.06% C - 0.6% Si - 0.2% S - 8.4% Ni - 18.2% Cr.

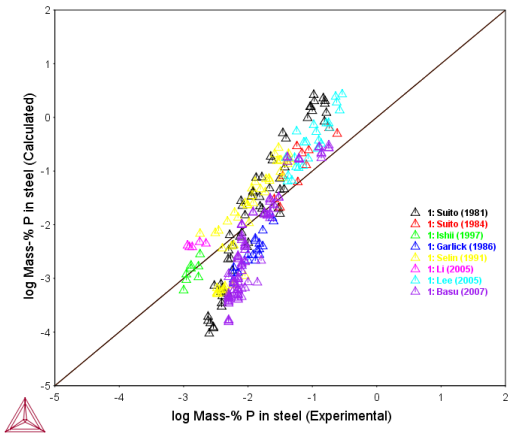

Figure 15: Comparison of experimental and calculated phosphorus solubility in liquid iron in equilibrium with slag in the Ca-Fe-Mg-O-P-Si system [see Figure 15 References].

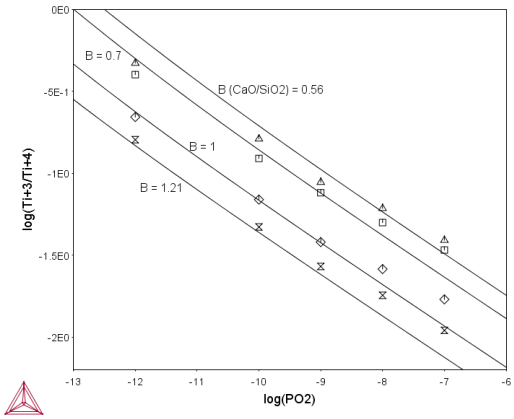

Figure 16: Variation of the Ti+3/Ti+4 ratio with oxygen partial pressure at 1600 °C with different CaO/SiO_2 ratios with experimental data [2002, Tranell].

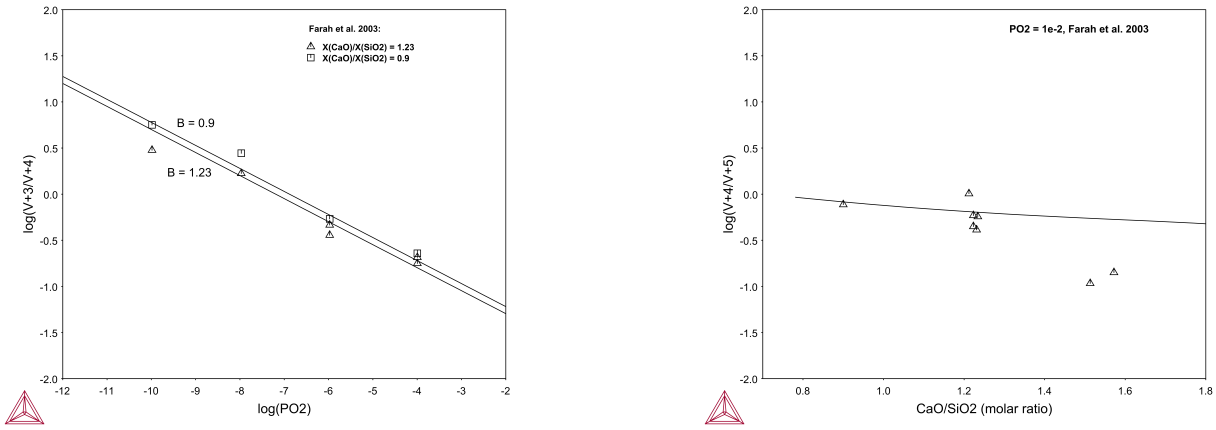

Figure 17: Variation of the V+3/V+4 ratio with oxygen partial pressure with different CaO/SiO_2 ratios (left) and V+4/V+5 ratio with basicity at a fixed oxygen partial pressure (right). Both calculated at 1600°C , with experimental data from [2003, Farah et al.].

Acknowledgement

Professor Malin Selleby, Dr. Bengt Hallstedt and David Dilner are acknowledged for many valuable discussions and important contributions.

TCOX9 References

[1956, Foster] P.K. Foster and A. J. E. Welch, “Metal-oxide solid solutions. Part 2. Activity relationships in solid solutions of ferrous oxide and manganous oxide,” Trans. Faraday Soc., vol. 52, 1636-1642, 1956.

[1960, Muan] A. Muan and S. Somiya, ”Phase Relations in the System Iron Oxide-Cr2O3 in Air. J. Am. Ceramic Soc., vol. 43(4), 204–209, 1960.

[1964, Bergstein] A. Bergstein and P. Kleinert, “Partial phase diagram of the system MnxFe3-xOy,” Collect. Czechoslov. Chem. Commun., vol. 29(10), 2549–2551, 1964.

[1965, Tretjakov] J.D. Tretjakov, Y.G. Saksonov, and I.V. Gordeev, "Chromite, Ferrite, Almninate,” Izv. Akad. Nauk. SSSR, Neorg. Mater., vol. 1, pp. 413-418, 1965.

[1966, Greskovich] C. Greskovich and V.S. Stubican, “Divalent chromium in magnesium-chromium spinels,” J. Phys. Chem. Solids, vol. 27(9), 1379–1384, 1966.

[1967, Schwerdt] K. Schwerdt and A. Muan, “Equilibria in System Fe-Mn-O Involving (Fe, Mn) O and (Fe, Mn) 3O4 Solid Solutions,” Trans. Metall. Soc. AIME, vol. 239(8), 1114–1119, 1967.

[1971, Ono] K. Ono, T. Ueda, T. Ozaki, Y. Ueda, A. Yamaguchi, and J. Moriyama, “Thermodynamic Study of the Fe-Mn-O System,” (in Japanese). Nippon Kinzoku Gakkai-Si, 38(8), 757–763, 1971.

[1975, Duquesnoy] A. Duquesnoy, J. Couzin, and P. Gode, “Isothermal Representation of Ternary Phase Diagrams ABO. Study of the System Mn-Fe-O,“ CR Acad. Sci. Paris C, vol. 281, 107–109, 1975.

[1980, Ono] K. Ono and T. Kohno, “Effect of Inclusion Composition on Stability of Inclusions and Corrosion Resistance of 18-8 Stainless Steel,” (in Japanese), Denki-Seiko, vol. 51, 122-131, 1980.

[1984, Ozturk] B. Ozturk and E.T. Turkdogan, “Equilibrium S distribution between molten calcium aluminate and steel, “Metal. Sci., vol. 18(6), 299-305, 1984.

[1985, Hillert] M. Hillert, B. Jansson, B. Sundman, and J. Ågren, “A two-sublattice model for molten solutions with different tendency for ionization,” Metall. Trans. A, vol. 16(1), 261–266, 1985.

[1987, Falke] H. Falke, Universität Hannover, Doctoral Thesis, 1987.

[1990, Franke] P. Franke and R. Dieckmann, “Thermodynamics of iron manganese mixed oxides at high temperatures,” J. Phys. Chem. Solids, vol. 51(1), 49–57, 1990.

[1991a, Sundman] B. Sundman, “Modification of the two-sublattice model for liquids,”Calphad, vol. 15(2), 109–119, 1991.

[1991b, Sundman] B. Sundman, “An assessment of the Fe-O system,” J. Phase Equilibria, vol. 12(2), 127–140, 1991.

[1993, Yin] Y. Yin and B.B. Argent, “The phase diagrams and thermodynamics of the ZrO2-CaO-MgO and MgO-CaO systems,” J. Phase Equilibria, vol. 14(5), 588–600, 1993.

[2001, Hillert] M. Hillert, “The compound energy formalism,” J. Alloys Compd., vol. 320(2), 161–176, 2001.

[2002, Tranell] G. Tranell, O. Ostrovski, and S. Jahanshahi, “The equilibrium partitioning of Titatium between Ti^{+3} and Ti^{+4} valency states in CaO-SiO_2-TiO_x slags”, Met Mater Trans B, vol. 33B, 61-66, 2002.

[2003, Farah] H. Farah, and M. Brungs, “Oxidation-reduction equilibria of vanadium in CaO-SiO_2, CaO-Al_2O_3-SiO_2 and CaO-MgO-SiO_2 melts“, J. Mater. Sci., vol. 38, 1885-1894, 2003.

[2006, Mao] H. Mao, M. Hillert, M. Selleby, and B. Sundman, “Thermodynamic Assessment of the CaO-Al2O3-SiO2 System,” J. Am. Ceramic Soc., vol. 89(1), 298–308, 2006.

[2008, Kjellqvist] L. Kjellqvist, M. Selleby, and B. Sundman, “Thermodynamic modelling of the Cr–Fe–Ni–O system, “Calphad, vol. 32(3), 577–592, 2008.

[2010, Kjellqvist] L. Kjellqvist and M. Selleby, ”Thermodynamic Assessment of the Fe-Mn-O System,” J. Phase Equilibria Diffus., vol. 31(2), 113–134, 2010.

[2013, Piao] R. Piao, H. Lee, and Y. Kang, “Experimental investigation of phase equilibria and thermodynamic modeling of the CaO–Al2O3–CaS and the CaO–SiO2–CaS oxysulfide systems,” Acta Mater., vol. 61(2), 683-696, 2013.

[2016, Allertz] C. Allertz, “Sulfur and Nitrogen in Ladle Slag”, PhD. thesis, KTH Royal Institute of Technology, Stockholm, Sweden, 2016.

[2016a, Poerschke] D.L. Poerschke, T.L. Barth, O. Fabrichnaya, and C.G. Levi, “Phase equilibria and crystal chemistry in the Calcia-Silica-Yttria system,” J. Eur. Ceram. Soc., vol. 36(7), 1743-1754, 2016.

[2016b, Poerschke] D.L. Poerschke, T.L. Barth, and C.G. Levi, “Equilibrium relationships between thermal barrier oxides and silicate melts,” Acta Mater., vol. 120, 302-314, 2016.

[2017, Poerschke] D.L. Poerschke and C.G. Levi, “Phase equilibria in the Calcia-Gadolinia-Silica system,“ J. Alloys Compd., vol. 695, 1397-1404, 2017.

Figure 9 References

[1929, Ruff] O. Ruff, F. Ebert, and E. Stephan,”Beiträge zur Keramik hochfeuerfester Stoffe II. Das System ZrO2-CaO,” Zeitschrift fur Anorg. und Allg. Chemie, vol. 180(1), 215–224, 1929.

[1933, Ebert] F. Ebert and E. Cohn, “Beiträge zur Keramik hochfeuerfester Stoffe. VI. Das System ZrO2-MgO,” Zeitschrift fur Anorg. und Allg. Chemie, vol. 213(4), 321–332, 1933.

[1940, Zhirnova] N. Zhirnova, Zh. Prikl. Khim. 12, pp. 1278, 1940.

[1959, Cocco] A. Cocco, “Composition Limits at High Temperatures of the Cubic Phase Composed of ZrO 2 and CaO,” Chim. Ind.(Milan), vol. 41(9), 882–886, 1959.

[1962, Hinz] I. Hinz, A. Dietzel, and H. Meyer, “Die Phasengrenze der kubischen ZrO2-MgO-Mischkristalle von 1800 C bis zum Schmelzpunkt,” Ber. Dtsch. Keram. Ges, 39, 530–533, 1962.

[1962 Tien] T.Y. Tien and E.C. Subbarao, ”X-Ray and Electrical Conductivity Study of the Fluorite Phase in the System ZrO2[Single Bond]CaO,” J. Chem. Phys., vol. 39(4), 1041, 1963.

[1965, Viechnicki] D. Viechnicki and V.S. Stubican, “Mechanism of Decomposition of the Cubic Solid Solutions in the System ZrO2-MgO,” J. Am. Ceram. Soc., vol. 48(6), 292–297, 1965.

[1967, Grain] C.F. Grain, “Phase Relations in the ZrO2-MgO System,” J. Am. Ceram. Soc., vol. 50(6), 288–290, 1967.

[1967, Noguchi] T. Noguchi, M. Mizuno, and W.M. Conn, “Fundamental research in refractory system with a solar furnace—ZrO2-CaO system,” Solar Energy, vol. 11(3-4), 145–152, 1967.

[1968, Garvie] R.C. Garvie, “The Cubic Field in the System CaO-ZrO 2,” J. Am. Ceram. Soc., vol. 51(10), 553–556, 1968.

[1968, Noguchi] T. Noguchi and M. Mizuno, “Liquidus Curve Measurements in the ZrO2-MgO System with the Solar Furnace,” Bull. Chem. Soc. Jpn., vol. 41(7), 1583–1587, 1968.

[1969, Traverse] J.P. Traverse and M. Foex, “The Zirconia–Strontia and Zirconia–Lime Systems,” High Temp. High Press., vol. 1(4), 409–427, 1969.

[1973, Michel] D. Michel, “Etats d’ordre dans la solution solide de type fluorite du systeme zircone - chaux pour la composition 4 ZrO2 – CaO,” Mater. Res. Bull., vol. 8(8), 943–949, 1973.

[1974, de Aza] S.D. de Aza, C. Richmond and J. White, “Compatibility Relationships of Periclase in System CaO-MgO-ZrO2-SiO2,” Trans. J. Br. Ceram. Soc., vol. 73(4), 109–116, 1974.

[1977, Stubican] V. S. Stubican and S.P. Ray, “Phase Equilibria and Ordering in the System ZrO2-CaO,” J. Am. Ceram. Soc., vol. 60(11-12), 534–537, 1977.

[1983, Hellmann] J.R. Hellmann and V.S. Stubican, “Phase Relations and Ordering in the Systems Mg0-Y203-Zr02 and Ca0-Mg0-ZrO,” J. Am. Ceram. Soc., vol. 66(4), 260–264, 1983.

[1987, Duran] P. Duran, P. Recio, and J.M. Rodriguez, “Low temperature phase equilibria and ordering in the ZrO2-rich region of the system ZrO2-CaO,” J. Mater. Sci., vol. 22(12), 4348–4356, 1987.

[1987, Sim] S. M. Sim and V. S. Stubican, “Phase Relations and Ordering in the System ZrO2-MgO,” J. Am. Ceram. Soc., 70(7), 521–526, 1987.

[1993, Yin] Y. Yin and B.B. Argent “Phase diagrams and thermodynamics of the systems ZrO2-CaO and ZrO2-MgO,” J. Phase Equilibria, vol. 14(4), 439–450, 1993.

Figure 15 References

[1981, Suito] H. Suito, R. Inoue and M. Takada, "Phosphorus distribution between liquid iron and Mgo saturated slags of the system CaO-MgO-FeOx-SiO2", Trans. Iron Steel Inst. Japan, vol. 21, 250-259, 1981.

[1984, Suito] H. Suito and R. Inoue, "Phosphorus distribution between Mgo saturated CaO-FeOx-SiO2-P2O5-MnO slags and liquid iron", Trans. Iron Steel Inst. Japan, vol. 24, 40-46, 1984.

[1986, Garlick] C. Garlic, S. Jahanshahi and G.R. Belton, unpublished work, BHP Central Research Laboratories, Shortland, Australia, 1986 (cited in Chen et al., 2013)

[1991, Selin] R. Selin, "Studies on MgO solubility in complex steelmaking slags in equilibrium with liquid iron and distribution of phosphorus and vanadium between slag and metal at MgO saturation", Scand. J. Metall., vol 20, 279-299, 1991.

[1997, Ishii] H. Ishii and R.J. Fruehan, "Dephosphorization equilibria between liquid iron and highly basic CaO-based slags saturated with MgO", Iron Steelmaking, vol 24, 47-54, 1997.

[2005, Li] G. Li, T. Hamano and F. Tsukihashi, "The effect of Na2O and Al2O3 on dephosphorization of molten steel by high basicity MgO saturated CaO-FeOx-SiO2 slag", ISIJ Int., vol 45, 12-18, 2005.

[2005, Lee] C.M. Lee and R.J. Fruehan, "Phosphorus equilibrium between hot metal and slag", Ironmaking Steelmaking Process. Prod. Appl., vol 32, 503-508, 2005.

[2007, Basu] S. Basu, A.K. Lahiri and S. Seetharaman, "Phosphorus partition between liquid steel and CaO-SiO2-P2O5-MgO slag containing low FeO", Metall. Mater. Trans. B, vol 38, 357-366, 2007.

[2013, Chen] Chen, L. Zhang and J. Lehmann, "Thermodynamic modelling of phosphorus in steelmaking slags", High Temp. Mater. Process., vol 32, 237-246, 2013.

Phases Included in TCOX9

In total there are 382 phases in the TCOX9 database.

When using Console Mode, phases and constituents can be listed in the DATABASE (TDB) module and the Gibbs (GES) module. To show models and constituents for the phases in a chosen system, use the command LIST_SYSTEM with the option CONSTITUENTS in the TDB module.

The Liquid Solution

The liquid phase contains all elements in the TCOX9 database except Ar. The ionic two-sublattice liquid model is used. The model may thus be used to describe liquid metal, oxides, sulfides, sulfur, fluoride, silicates etc. with the following formula:

$(Al^{+3}, Ca^{+2}, Co^{+2}, Cr^{+2}, Cu^{+1}, Fe^{+2}, Gd^{+3}, La^{+3}, Mg^{+2}, Mn^{+2}, Mo^{+4}, Nb^{+2}, Ni^{+2}, P^{+5}, Si^{+4}, Ti^{+2}, V^{+2}, W^{+6}, Y^{+3}, Zr^{+4})_P$ $(AlO_2^{-1}, F^{-1}, O^{-2}, PO_4^{-3}, S^{-2}, SiO_4^{-4}, SO_4^{-2}, Va, C, C_3S_2Z_{1/6}, CoF_3, CoO_{3/2}, CrF_3, CrO_{3/2}, CuF_2, CuO, FeF_3, FeO_{3/2}, M_3S_2Z_{1/6}, MnO_{3/2}, NbF_5, NbO_2, NbO_{5/2}, PO_{5/2}, S, SiO_2, TiO_{3/2}, TiO_2, VO_2, VO_{3/2}, VO_{5/2})_Q$

Alloy Phases

BCC_A2

Containing Al, Ca, Co, Cr, Cu, Fe, Gd, La, Mg, Mn, Mo, Nb, Ni, P, S, Si, Ti, V, W, Y and Zr with C and O modeled interstitially.

FCC_A1

Containing Al, Ca, Co, Cr, Cu, Fe, Gd, La, Mg, Mn, Mo, Nb, Ni, P, S, Si, Ti, V, W, Y and Zr with C and O modeled interstitially. FCC_A1 also describes cubic carbides and the two cubic oxides TiO and VO solid solutions.

HCP_A3

Containing Al, Ca, Co, Cr, Cu, Fe, Gd, La, Mg, Mn, Mo, Nb, Ni, Si, Ti, V, W, Y and Zr with C and O modeled interstitially.

DHCP

La phase dissolving Al, Ca, Cu, Gd, Mg, Mn, Ni and Y with O modeled interstitially.

CUB_A13

β-Mn, containing Al, Co, Cr, Fe, Mg, Mo, Nb, Ni, Si, Ti, V and Zr with C modeled interstitially.

CBCC_A12

α-Mn, containing Al, Co, Cr, Fe, Mg, Mo, Nb, Ni, Si, Ti, V and Zr with C modeled interstitially.

DIAMOND_FCC_A4

Diamond structure based on Si containing Al, C and P with O modeled interstitially.

GRAPHITE

This is pure carbon.

RED_P, WHITE_P

This is pure phosphorus. Phosphorus exists in two modifications: white (not stable at normal conditions) and red (up to the melting temperature of 579° C).

ORTHORHOMBIC_S, MONOCLINIC_S

This is pure sulfur. Sulfur exists in two modifications: orthorhombic (up to 95° C) and monoclinic (up to the melting temperature of 115° C).

Gas Phase

A reduced gas phase containing AL1F3, AR, C1O1, C1O2, CA1F2, F, F2, O, O10P4, O1P1, O2P1, O1S1, O2, O2S1, O3S1, O5P2, O1TI1, P2, P4, S2, and Ti.

Solid Solutions

The solid solution phases are modeled within the framework of the Compound Energy Formalism (CEF) [3]. These models take into account distribution of cations between sublattices, defects such as vacancies, anti-sites and ordering. 145 solutions are modeled in the database.

Alabandite

This is CaS (oldhamite), MnS (alabandite), MgS, GdS, LaS and ZrS solid solution.

$AlPO_4$

There are three modifications (S1, S2 and S3)of $AlPO_4$ with solubility of SiO_2.

α-Spinel

This is low-temperature tetragonal Mn_3O_4 solid solution dissolving Al, Co, Cr, Cu, Fe, Mg and Ni. Distribution of cations between tetrahedral and octahedral sites, as well as vacancies on the octahedral sites to model deviation from the ideal stoichiometry toward higher oxygen potential and interstitial Mn to model deviation toward excess manganese are taken into account.

Anhydrite

This is (Ca,Cu,Fe,Mg,Mn,Ni)SO_4.

Apatite

This is $(Ca,Mg)_2(Gd,Y)_8(SiO_4)_6O_2$ solid solution dissolving Zr.

β-V-O

This is β-V-O.

Bronze

This is $(Ca,Fe)_xV_2O_5$ bronze.

Calcium ferro-aluminates

- C3A1: This is $Ca_3Al_2O_6$ dissolving ferric Fe.
- C12A7: This is $Ca_{12}Al_{14}O_{32}$ dissolving ferric Fe. C12A7 is not stable in the anhydrous CaO-Al_2O_3 system. It is, however, important in practice, and included in the database. In the optimization it was treated as if it does not contain any water.
- C1A1: This is $CaAl_2O_4$ dissolving ferric Fe.
- C1A2: This is $CaAl_4O_7$ dissolving ferric Fe.
- C1A6: This is $CaAl_{12}O_{19}$ dissolving ferric Fe.
- C1A1F2: This is $Al_2CaFe_4O_{10}$ with a variation in Al/Fe: $CaAlFe_2(Al,Fe)_3O_{10}$.
- C2F: This is $Ca_2Fe_2O_5$ dissolving Al.

$Ca_3P_2O_8$ (α and β)

α-$Ca_3P_2O_8$ dissolving Mg and Si and β-$Ca_3P_2O_8$ dissolving Mg.

$Ca_2P_2O_7$ (α, β and γ)

α, β and γ-$Ca_2P_2O_7$ dissolving Mg.

Ca_2SiO_4 (α and α')

α-Ca_2SiO_4- α'-$Ca_3P_2O_8$ dissolving Gd, Mg, Mn, Y and α'-Ca_2SiO_4 dissolving Fe, Gd, Mg, Mn, P and Y.

$Ca_3S_3Fe_4O_x$

This is the oxy-sulfide 3CaS.4FeO-3CaS.$4Fe_2O_3$.

$Ca_3Y_2Si_3O_{12}$

This is $Ca_3(Gd,Y)_2(SiO_4)_3$.

$Ca_3Y_2Si_6O_{18}$

This is $Ca_3(Gd,Y)_2(SiO_4)_6$.

$Ca_4Nb_2O_9$_HT11

This is the high-temperature $Ca_4Nb_2O_9$ phase with excess CaO.

$Ca_4Nb_2O_9$_LT21

This is the low-temperature $Ca_4Nb_2O_9$ phase with excess CaO.

$Ca_3Co_2O_6$

This is $Ca_3Co_2O_6$ dissolving Cu.

$Ca_3Co_4O_9$

This is $Ca_3Co_4O_9$ dissolving Cu.

$CaCr_2O_4$_A

This is the high-temperature $CaCr_2O_4$ dissolving Al and Fe.

CaF_2_S1

This is low-temperature CaF_2 dissolving CaO and MgF_2.

CaF_2_S2

This is high-temperature CaF_2 and CuF_2 dissolving CaO and MgF_2.

$Ca_3Mg_3P_4O_{16}$

This is $Ca_3Mg_3P_4O_{16}$.

$CaMO_3$

This is $CaMnO_3$, $CaTiO_3$ and low-temperature $CaZrO_3$ dissolving Y.

$Ca_5P_2SiO_{12}$

This is $Ca_5P_2SiO_{12}$.

CaSFeO

This is the oxy-sulfide CaS.FeO-$CaS.Fe_2O_3$.

$CaSO_4$_HT

This is (Ca,Co,Mg)SO_4.

CaV_2O_4

This is $CaFe_2O_4$, β-$CaCr_2O_4$, CaV_2O_4 and CaY_2O_4 solid solution dissolving Al. Prototype phase is CaV_2O_4.

CaV_2O_6

This is (Ca,Co,Mg,Mn,Ni)V_2O_6.

CaY_4O_7

This is Ca(Gd,Y)$_4O_7$.

$CaYAl_3O_7$

This is Ca(Gd,Y)Al_3O_7.

$CaYAlO_4$

This is Ca(Gd,Y)AlO_4.

$CaZrO_3$_C

This is the cubic high-temperature $CaZrO_3$ phase dissolving Y.

Chalcopyrite

This is an intermediate solid solution phase in the Cu-Fe-S system around the composition $CuFeS_2$.

Co_9S_8

This is Co_9S_8 dissolving Fe and Ni.

Columbite

This is (Ca,Co,Fe,Mg,Mn)Nb_2O_6 with excess FeO and MgO.

Cordierite

This is Al_4(Fe,Mg,Mn)$_2Si_5O_8$.

Corundum

This is Corundum (Al_2O_3), Eskolaite (Cr_2O_3), Hematite (Fe_2O_3), Karelianite (V_2O_3), Tistarite (Ti_2O_3) and (Co,Fe,Mg,Mn,Ni)TiO_3 Ilmenite solid solution.

Cr_2S_3

This is Cr_2S_3 dissolving Fe.

Cr_3S_4

This is Cr_3S_4 dissolving Fe, Mn and Ni.

$CrNbO_4$

This is $CrNbO_4$ solid solution with excess Cr_2O_3 and Nb_2O_5.

$Cr_2P_4O_{13}$

This is $Cr_2P_4O_{13}$ and $(Cr,Fe)_2V_4O_{13}$.

$Cr_2Ti_2O_7$

This is $Cr_2Ti_2O_7$ with solubility of Al and Fe.

CuF_2

This is CrF_2 and low temperature CuF_2.

$CuLa_2O_4$

This is $CuLa_2O_4$ with solubility of Co.

CuP_2O_6

This is $(Co,Cu,Ni)P_2O_6$.

CuO

This is CuO with solubility of Co.

Cristobalite

This is SiO_2 with solubility of $AlPO_4$.

Delafossite

This is $Cu(Al,Cr,Fe,La,Mn,Y)O_2$.

Digenite

This is Cu_2S solid solution with excess S and solubility of Fe, Mg and Mn.

$DyMn_2O_5$

This is $Mn_2(Gd,Y)O_5$ solid solution. Prototype phase is $DyMn_2O_5$.

FeF_3

This is $(Al,Co,Cr,Fe)F_3$.

$Fe_2O_{12}S_3$

This is the oxy-sulfides $(Al,Cr,Fe)_2(SO_4)_3$.

$FeNb_{14}O_{36}$

This is $(Co,Fe)Nb_{14}O_{36}$.

$FeNb_{36}O_{91}$

This is $(Co,Fe)Nb_{36}O_{91}$.

$FeNb_{68}O_{171}$

This is $(Co,Fe)Nb_{68}O_{171}$.

$FePO_4$

This is $(Fe,Mn)PO_4$.

$FeVO_4$

This is $(Al,Fe)VO_4$.

Fluorite

This is high-temperature ZrO_2 solid solution with solubility of Al, Ca, Cr, Fe, Gd, La, Mg, Mn, Ni, Si, Ti and Y.

Garnet

This is grossular ($Ca_3Al_2Si_3O_{12}$), uvarovite ($Ca_3Cr_2Si_3O_{12}$), spessartine ($Mn_3Al_2Si_3O_{12}$), and goldmanite ($Ca_3V_2Si_3O_{12}$).

GdF_3

This is high temperature $(Gd,Y)F_3$.

$Gd_2Si_2O_7$

This is $(Gd,La)_2Si_2O_7$.

Gd_2SiO_5

This is $(Gd,La)_2SiO_5$.

Halite

This is Lime (CaO), CoO, Wustite (FeO), Periclase (MgO), Manganosite (MnO), bunsenite (NiO) solid solution dissolving also Al, Cu, Cr, Gd, Ti, V, Y and Zr.

Hatrurite

This is Ca_3SiO_5 dissolving Gd and Y.

β1-Heazlewoodite

This is non-stoichiometric high-temperature Ni_3S_2 dissolving Co and Fe.

β2-Heazlewoodite

This is non-stoichiometric high-temperature Ni_4S_3 dissolving Fe.

LaF_3

This is low temperature $(Gd,La,Y)F_3$.

La_2S_3

This is $(Gd,La)_2S_3$.

La_2MnO_4

This is $La_2(Mn,Ni)O_4$ solid solution dissolving Co.

$La_3Ni_2O_7$

This is $La_3Ni_2O_7$ dissolving Co.

$La_4Ni_3O_{10}$

This is $La_4Ni_3O_{10}$ dissolving Co.

LaAP

This is a rhombohedral perovskite, $La(Al,Co)O_3$ dissolving Ca, Cu, Ni and Y.

LaYP

This is the orthorhombic perovskite, $LaYO_3$ solid solution.

α-M_2O_3

This is hexagonal α-La_2O_3 and Gd_2O_3 solid solution dissolving Ca, Mg, Y and Zr.

β-M_2O_3

This is monoclinic β-Gd_2O_3 dissolving Al, Ca, Co, La, Mg, Y and Zr.

c-M_2O_3

This is Mn_2O_3, cubic Gd_2O_3 and Y_2O_3 solid solution dissolving Al, Ca, Co, Cr, Fe, La, Mg, Ni, Ti, Y and Zr.

h-M_2O_3

This is hexagonal La_2O_3, Gd_2O_3 and Y_2O_3 solid solution dissolving Ca, Mg, Mn and Zr.

x-M_2O_3

This is x-La_2O_3 and high-temperature cubic Gd_2O_3 solid solution dissolving Ca, Mg, Y and Zr.

M_4O_7

This is $(Ti,V)_4O_7$ solid solution dissolving Al and Mn.

M_6O_{11}

This is $(Ti,V)_6O_{11}$ solid solution.

M_7O_{13}

This is $(Ti,V)_7O_{13}$ solid solution.

Melilite

This is Gehlenite ($Ca_2Al_2SiO_7$), Fe-Gehlenite ($Ca_2Fe_2SiO_7$), Åkermanite (Ca_2MgSiO_7), Fe-Åkermanite (Ca_2FeSiO_7) and $Ca_2CoSi_2O_7$.

MgF_2

This is $(Co,Fe,Mg,Mn,Ni,V)F_2$.

$Mg_2P_2O_7$ (α and β)

This is α and β-$Mg_2P_2O_7$ dissolving Ca.

$Mg_2V_2O_7$

This is $(Co,Mg,Ni)_2V_2O_7$.

$Mg_3P_2O_8$

This is $Mg_3P_2O_8$ dissolving Ca.

$Mg_3V_2O_8$

This is $(Co,Mg,Ni)_3V_2O_8$.

$MgWO_4$-type

This is $(Al,Fe)NbO_4$ and $(Co,Fe,Mg,Mn,Ni)WO_4$ solid solution. Prototype $MgWO_4$.

$Mn_4Nb_2O_9$

This is $(Co,Fe,Mg,Mn)_4Nb_2O_9$.

MoS_2

This is $(Mo,W)S_2$ solid solution.

Mullite

Mullite (around $Al_6Si_2O_{13}$) solid solution dissolving Fe.

NbO_2

This is NbO_2 dissolving Fe.

Nb_2O_5

This is Nb_2O_5 dissolving Mg and V.

Ni_6MnO_8-type

This is $(Mg,Ni)_6MnO_8$.

Ni_7S_6

This is Ni_7S_6 dissolving Fe.

Ni_9S_8

This is Ni_9S_8 dissolving Fe.

$NiMnO_3$

This is $NiMnO_3$ with Ilmenite structure.

$NiNb_2O_6$

This is $NiNb_2O_6$. This phase has the same structure as the Nb_2FeO_6 phase, but is modeled separately.

Olivine

This is Calcio-olivine (Ca_2SiO_4) – Co_2SiO_4 – Fayalite (Fe_2SiO_4) – Forsterite (Mg_2SiO_4) – Tephroite (Mn_2SiO_4) – Ni_2SiO_4 – Kirschsteinite ($CaFeSiO_4$) – Monticellite ($CaMgSiO_4$) solid solution dissolving Cr and Cu.

Pentlandite

This is ternary $(Fe,Ni)_9S_8$.

Perovskite

This is $(Cr,Fe,Mn)LaO_3$.

Pseudo-brookite

This is Fe_2TiO_5. This is also Ti_3O_5, Al_2TiO_5 and $(Co,Fe,Mg,Mn)Ti_2O_5$ with solubility of Ni and V.

Pyrite

This is Cattierite (CoS_2), Pyrite (FeS_2) – Hauerite (MnS_2) – Vaesite (NiS_2).

Pyrochlore

This is $(Gd,La)_2Zr_2O_7$ and $(Gd,La,Y)_2Ti_2O_7$ solid solution dissolving Y.

Pyroxenes

Modeling of low clino-pyroxene, clino-pyroxene, ortho-pyroxene and proto-pyroxene solid solutions taking into account the distribution of cations between different sublattices.

- Low clino-pyroxene: This is low clino-enstatite ($MgSiO_3$) and low clino-diopside ($CaMgSi_2O_6$).
- Clino-pyroxene: This is clino-enstatite ($MgSiO_3$), clino-ferrosilit ($FeSiO_3$), diopside ($CaMgSi_2O_6$), niopside ($CaNiSi_2O_6$), pigeonite ($(Mg,Fe,Ca)Si_2O_6$), hedenbergite ($CaFeSi_2O_6$) dissolving Co.
- Ortho-pyroxene: This is enstatite ($MgSiO_3$) and ortho-diopside ($CaMgSi_2O_6$) with Fe solubility.
- Proto-pyroxene: This is proto-enstatite ($MgSiO_3$) and proto-diopside ($CaMgSi_2O_6$) dissolving Co, Cr and Fe.

Pyrrhotite

This is Pyrrhotite (FeS) – CoS – CrS– NbS – NiS – TiS – VS solid solution dissolving Al, Cu, Gd, Mg, Mn and Zr.

Quartz

This is SiO_2 with solubility of $AlPO_4$.

Rhodonite

This is $MnO.SiO_2$ dissolving Ca, Co, Fe and Mg.

Rutile

This is MnO_2 – TiO_2 – high temperature VO_2 solid solution dissolving Al and Zr.

Spinel

This is the cubic AB_2O_4-type spinel solid solution containing Al-Ca-Co-Cr-Cu-Fe-Mg-Mn-Ni-Ti-O. Distribution of cations between tetrahedral and octahedral sites, as well as vacancies on the octahedral sites to model deviation from the ideal stoichiometry toward higher oxygen potential and interstitial Fe to model deviation toward excess iron are taken into account.

This is Spinel ($MgAl_2O_4$), Magnetite (Fe_3O_4), Cuprospinel ($CrFe_2O_4$), Hercynite ($FeAl_2O_4$) and many more.

Thio-spinel

This is the sulfur spinel. This has the same structure as the oxygen-spinel, but is modeled as a separate phase. This is $(Cu,Fe,Mn)Cr_2S_4$ – Co_3S_4 – $FeNi_2S_4$ – Ni_3S_4.

Ti_5O_9

This is Ti_5O_9 dissolving V.

Tridymite

This is SiO_2 with solubility of $AlPO_4$.

V_2O_SS

This is V_2O solid solution.

V_3O_5-HT

This is high temperature V_3O_5 dissolving Al, Cr, Mn and Ti.

V_5O_9

This is V_5O_9 dissolving Ti.

VO_2-LT

This is low temperature VO_2, MoO_2 and WO_2.

Wollastonite

This is $CaSiO_3$ dissolving Fe, Mg and Mn.

YAG

This is $(Gd,Y)_3(Al,Fe)_5O_{12}$ solid solution dissolving Cr and La.

YAM

This is $(Gd,Y)_4Al_2O_9$ and Cuspidine ($Ca_2Y_2Si_2O_9$) solid solution dissolving La.

YAP

This is $(Gd,Y)(Al,Co,Cr,Fe)O_3$ solid solution dissolving Ca, Mn and La.

Y_2TiO_5

This is $(Gd,La,Y)_2TiO_5$ solid solution.

Y_3NbO_7

This is Y_3NbO_7 solid solution with excess Nb_2O_5 and Y_2O_3.

$YNbO_4$

This is $YNbO_4$ solid solution with excess Y_2O_3.

Zircon

This is Zircon ($ZrSiO_4$) and $(Gd,Y)PO_4$ solid solution.

m-ZrO_2

This is monoclinic ZrO_2 solid solution dissolving Al, Ca, Cr, Gd, La, Ti and Y.

t-ZrO_2

This is tetragonal ZrO_2 solid solution dissolving Al, Ca, Cr, Fe, Gd, La, Mg, Mn, Ni, Ti and Y.

β-$ZrTiO_4$

This is $ZrTiO_4$ with solubility of Al.

Stoichiometric Compounds

223 stoichiometric compounds are modeled in the TCOX9 database.

AF
AL2P6SI4O26
AL2S3
AL2SIO4F
AL3PO7
ALF3_S2
ALNB11O29
ALNB49O124
ALP3O9
ANDALUSITE
ANILITE
ANORTHITE
C11A7F
C13A6Z2
C1A8M2
C2A14M2
C3A2M1
C3A3F
C4WF4
C4WF8
CA10P6O25
CA10SI3O15F2
CA10V6O19
CA15CU18O35
CA2ALNBO6
CA2CUO3
CA2NB2O7
CA2P6O17
CA2V2O7
CA2ZRSI4O12
CA3COAL4O10
CA3NB2O8
CA3TI2O7
CA3TI8AL12O37
CA3V2O8
CA3WO6
CA3ZRSI2O9
CA4MG2P6O21
CA4P2O9_A
CA4P2O9_B
CA4P6O19
CA4TI3O10
CA4V2O9
CA5SI2O8F2
CA6ZR19O44
CA7P2SI2O16
CA9V6O18
CACRSI4O10
CACU2O3
CAMG3O16S4
CAMN2O4
CAP2O6_A
CAP2O6_B
CAP2O6_G
CAP4O11_A
CAP4O11_B
CAV2O5
CAV3O7
CAV4O9

CAVO3
CAWO4
CAZR4O9
CF2
CHALCOCITE_ALPHA
CHALCOCITE_BETA
CO1LA2O4
CO2P2O7
CO3LA4O10
CO3P2O8
COVELLITE
CR1S1
CR3P2O8
CR3PO7
CR4P6O21
CR5PO10
CR5S6
CR7S8
CRNB25O64
CRNB49O124
CRNB9O24
CRP3O9
CRPO4
CRVO4
CU2COO3
CU2P2O7
CU2SO4
CU2SO5
CU2Y2O5
CU3NB2O8
CU3P2O8
CUCRS2
CUF
CUFES2_LT
CUGD2O4
CUNB2O6
CUPO3
CUPRITE
CUSPIDINE
CW3F
CWF
DJURLEITE
FE18P2O24
FE2P2O7
FE2PO5
FE3P2O8
FE3P4O14
FE3PO7
FE4P6O21
FE7P6O24
FE7P8O28
FEAL2S4
FENB25O64
FENB49O124
FENB9O24
FEP2O6
FEP3O9
FEV2O6
GUGGENITE
KYANITE
LA1S2
LA2CR3O12
LA2CRO6

LA2NB12O33

LA2TI3O9
LA3NBO7
LA4SI3O12
LA4TI3O12
LA4TI9O24
LAAL11O18
LAFE12O19
LANB3O9
LANBO4
LANIO3
LARNITE
MERWINITE
MG2NB34O87
MG5NB4O15
MGP2O6
MGP4O11
MN2P2O7
MN2V2O7
MN3P2O8
MN9SI3O14S1
MNF2_S1
MNF3
MNP2O6
MNYO3_HEX
MO2S3
MO4O11
MO8O23
MO9O26
MOF4
MOO3
NBF5
NBO

NI2P2O7
NI3P2O8
NI3S2_LT
NI4NB2O9
NINB14O36
NINB36O91
NINB68O171
NIOCALITE_C10NS6
NIS_LT
P2O5_H
P2O5_O
P2O5_OP
P2S5
PSEUDO_WOLLASTONITE
Q_ALMGZRO
RANKINITE
SAPPHIRINE
SI3P4O16
SILLIMANITE
SIP2O7_CUB
SIP2O7_MONO
SIP2O7_TETR
SIS2
SPHENE
TI10O19
TI20O39
TI2NB10O29
TI2S
TI3O2
TI5P6O25
TI8S10

TI8S3

TI8S9
TI9O17
TINB24O62
TINB2O7
TIO_ALPHA
TIP2O7
TIS2
TIS3
V2O5
V3O5_LT
V3O7
V52O64
V6O13
WO2_72
WO2_90
WO2_96
WO3_HT
WO3_LT
Y2S2A_Y2SI2O7
Y2S2B_Y2SI2O7
Y2S2D_Y2SI2O7
Y2S2G_Y2SI2O7
Y2SIO5
ZR11NB4O32
ZR13NB4O36
ZR15NB4O40
ZR3Y4O12
ZR5NB2O15
ZR6NB2O17
ZR7NB2O19
ZR8NB2O21

ZRF4
ZRO8S2
ZRS2
ZRTI2O6
ZRTIO4_ALPHA